DOI: 10.48011/asba.v2i1.1588

Modeling and Simulation of Energy Harvesting Technologies in Low Power Nanogrids

Jéssica P. Domingos * **Rodrigo A. F. Ferreira** *
Márcio C. B. P. Rodrigues * **Pedro G. Barbosa** **

* *Power Electronics and Applications Group, Federal Institute of Southeast of Minas Gerais, MG, (e-mail: rodrigo.ferreira@ifsudestemg.edu.br)*
** *Power Electronics and Automation Group, Federal University of Juiz de Fora, MG, (e-mail: pedro.gomes@ufjf.edu.br)*

Abstract: This work presents an analysis on the integration of energy harvesting technologies used for low power applications. The main goal is to develop a simulation platform representing a nanogrid using the consolidated models of three of the most mature energy harvest sources: photovoltaic, thermoelectric and piezoelectric. The resulting model is used to evaluate the advantages of adding energy harvesters to a battery supplied applicaiton. It will be presented a short literature review, as well as discussion about equivalent circuit models for each one of the sources used on the proposed 100 mW nanogrid. Aspects regarding modelling and simulation of the system on PSIM is presented and some case studies are performed to validate the proposed methodology.

Keywords: Piezoelectric; Photovoltaics; TEG; Simulation; Wearables.

1. INTRODUCTION

It is increasingly common to use sensors and other devices of low energy consumption in a variety of applications: from health monitoring and sports performance analysis to industrial, residential and automotive devices (Bandyopadhyay and Chandrakasan, 2012). Some of those devices, such as smartwatches or health monitoring apparatus need to be recharged in intervals of hours or days. In some applications, a small number of sensors nodes is used, forming a Wireless Sensor Network (WSN). In that case, sensor nodes have limited battery capacity, and multiple on-board sensors that can take readings, such as temperature and humidity (Shaikh and Zeadally, 2016). The WSN may be located in large number of sensors or in remote locations, making battery replacement extremely challenging (Bandyopadhyay and Chandrakasan, 2012).

The concept of Energy Harvesting comes as a way to increase the operating time of those devices as well as to increase the life of the batteries once the discharge cycle becomes longer. There are several sources of energy harvesting, such as: photovoltaic, thermoelectric, piezoelectric, among others (Shaikh and Zeadally, 2016; Raghunathan et al., 2005). Radio Frequency (RF) signals also can be used to generate electricity to ultra low power applications (Ramadass, 2009). Table 1 shows a summary for each of the most mature harvesting technologies mentioned above (Pozo et al., 2019). However, since the nature of generation of those sources is intermittent, it is interesting to use a combination of sources to achieve a better overall performance of the power system. Bjørk and Nielsen (2015) considered a combined Photovoltaic (PV) and Thermoelectric Generator (TEG) system, where the TEG is mounted directly on the back of the PV. Combination of PV, TEG and Piezoelectric Energy Harvester (PEH) is presented by Bandyopadhyay and Chandrakasan (2012).

Table 1. Summary of energy harvesting technologies.

Harvester	**Power Density**	**Maximum Efficiency**
Photovoltaic	0.01-15 mW/cm^2	40%
Piezoelectric	330 $\mu W/cm^2$	30%
Thermoelectric	0.1-100 mW/cm^2	15%
RF	0.01-0.1 $\mu W/cm^2$	60%

In general, applications using Energy Harvesting concept can be classified as Nanogrids. The term refers to at least one source, one load and some level of control and/or supervision. Energy Storage System (ESS) is not mandatory, but very common. The major difference between microgrid and nanogrid concept is that in the later one, in many cases, the power may be less than 1 W (Nordman, 2013).

Although the experimental setups of energy harvesting systems are relatively simple – there are even commercial development kits available – once they are strictly dependent on weather conditions and/or the environment in which the application is located, it is interesting to develop a platform for simulating such systems. Additionally, the platform can be useful for testing control and protection systems and to perform stability analysis of related applications.

Taking into the account the above, the present study aims to evaluate the advantages of adding energy harvesters to a battery supplied low power nanogrid using a simulation platform modeled in PSIM.

2. ENERGY HARVESTERS

2.1 Photovoltaic Generator

Photovoltaic based energy harvesting provides the highest power density so it becomes the main choice to power an embedded system that consumes several mW using a reasonably small harvesting module (Raghunathan et al., 2005).

The equivalent circuit of a photovoltaic cell is shown in Figure 1 (a) (Farret and Simões, 2006). The current source I_λ is dependent on Irradiance and Temperature of the cell. Since the PV cell is a p-n junction, its characteristics is similar of the one of a diode. Therefore, its Power-Voltage (PV) curve can be represented as shown on Fig 1 (b).

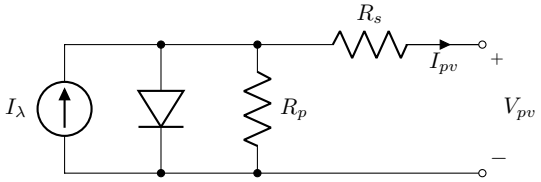

(a) Equivalent Circuit

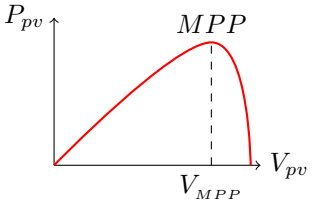

(b) P-V curve

Figure 1. Photovoltaic cell.

In most of applications it wants to maximize the power delivered from the photovoltaic cell, i.e., it is desired to operate at the Maximum Power Point (MPP) of the P-V curve.

Several methods of MPP Tracking (MPPT) can be found in literature, such as Perturb and Observe (P&O), Hill-Climbing (HC), Incremental Conductante (INC), among others (Hohm and Ropp, 2003; Rezk and Eltamaly, 2015).

In general, overall performance of the methods is at the same level. Some are more stable, some are more efficient and some are simpler to implement. Since this discussion goes beyond the scope of the work, information will be limited in the choice of the P&O method due to its rapid response and low error in steady state (Rezk and Eltamaly, 2015).

A DC-DC converter is needed in order to interconnect the PV cell and the main bus of the nanogrid and to perform the MPPT control. Since this work deals with a low power application with low converter gain requirement, a non-isolated converter will be used.

The use of a Buck-Boost topology (or one of its variations) is preferred because it is more appropriate to perform MPPT, mainly in situations which the environmental conditions ranges widely (Coelho et al., 2010).

2.2 Thermoelectric Generator

A thermoelectric generator consists of N pairs of p and n semiconductors, connected electrically in series and thermally in parallel (Siouane et al., 2017). A thermoelectric element converts thermal energy in the form of temperature differences into electrical energy (Seebeck effect) and vice-versa (Peltier effect) (Ramadass, 2009).

Different models of TEG can be found in the literature (Siouane et al., 2017). Considering an application with a constant temperature difference, the equivalent circuit of a TEG is shown in Figure 2 (Bandyopadhyay and Chandrakasan, 2012; Ramadass, 2009; Siouane et al., 2017).

The equivalent voltage source is given by (1).

$$V_{TEG} = \alpha \Delta T, \tag{1}$$

where α is the Seebeck coefficient, which depends on the thermoelectric materials and ΔT is the temperature difference.

The internal resistance R_{TEG} comprises the electrical resistance of the p-n semiconductors and contacts used to connect the TEG to an electrical load. R_{TEG} ranges from some $m\Omega$ to a few Ω (Siouane et al., 2017; Karami and Moubayed, 2014).

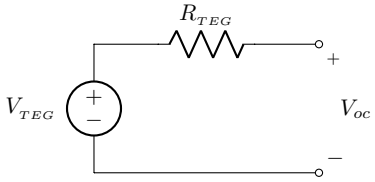

(a) Equivalent Circuit

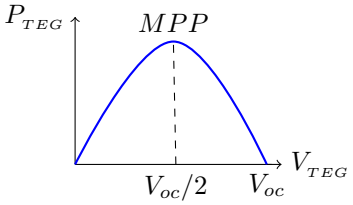

(b) P-V curve

Figure 2. Thermoelectric Generator.

Since equivalent circuit of TEG is a non-ideal voltage source, it is subject to the maximum power transfer theorem. The maximum power point occurs when the output voltage is equal to half of the equivalent voltage source.

As well as occurs in PV generation, it is possible to use some method for tracking the MPPP. A DC-DC converter is used to keep the output voltage of the TEG near to $V_{oc}/2$. However, there is an alternative mode to guarantee that the device will provide the maximum power. The reference voltage of the DC-DC converter is refreshed

from times to times opening the circuit and measuring its terminal voltage (Bandyopadhyay and Chandrakasan, 2012; Do et al., 2014).

2.3 Piezoelectric Energy Harvester

In some applications, the presence of vibrations makes it possible to harvest mechanical energy. Emerging implementations of Piezoelectric Energy Harvesting technology can be found in different application fields, such as wireless industrial monitoring, health monitoring, and automotive technology (Dell'Anna et al., 2018). An input vibration applied on to a piezoelectric material causes mechanical strain to develop in the device which is converted to electrical charge. On the other hand, the application of an electric voltage to this material produces a mechanical strain (Ramadass, 2009).

Piezoelectric structures generate an AC voltage that cannot be used directly to power most common low power applications. Hence, a rectifier circuit is needed as interface between PEH and the DC part of the circuitry (Dell'Anna et al., 2018). Voltage Doubler can be used either, in order to boost the output voltage of the structure (Bandyopadhyay and Chandrakasan, 2012; Ramadass, 2009; Dell'Anna et al., 2018).

The equivalent circuit of the PEH including the voltage doubler is shown in Figure 3 (a). $I_p sen(\omega t)$ represent the amplitude of the vibrations with frequency of ω. C_p and R_p models the parasitic elements of the piezoelectric device. The value of C_p is about a few nF, and R_p is in the range of hundreds of $k\Omega$ to a few $M\Omega$ (Ramadass, 2009; Dell'Anna et al., 2018).

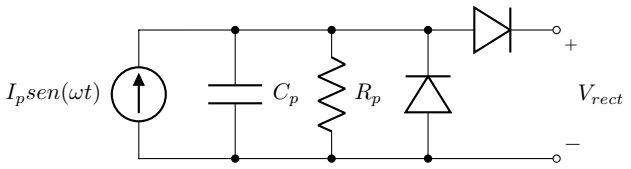

(a) AC Equivalent Circuit

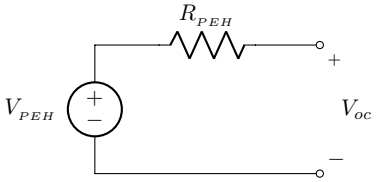

(b) DC Equivalent Circuit

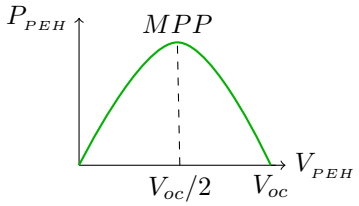

(c) P-V curve

Figure 3. Piezoelectric Energy Harvester.

The ac model of the piezoelectric harvester at resonance, along with the rectifier, is equivalent to a dc voltage source in series with a resistor as shown in Figure 3 (b) (Bandyopadhyay and Chandrakasan, 2012). The parameters is given by (2).

$$V_{eq} = \frac{2I_p}{\omega C_p}, \qquad (2)$$
$$R_{eq} = \frac{1}{C_p f}.$$

Similar to TEG devices, the maximum power point occurs when the output voltage is equal to half of the equivalent voltage source, as can be seen in Figure 3 (c). A DC-DC converter is also used to keep the output voltage of the TEG near to $V_{oc}/2$, using any of the MPPT methods or the alternative

3. DESCRIPTION OF THE MODEL

In this work, the concept of Nanogrid is used to combine sources, ESS and loads. The system was modeled in PSIM, and it is shown in Figure 4. The methodology consists of using PV generator, TEG and PEH as sources, a small battery as ESS and a combination of Constant Power Load (CPL) and Constant Impedance Load (CZL).

Parameters used in modeled circuit is summarized in Table 2.

Table 2. Model Parameters

Parameter	Value	Unit
$V_{PV,mpp}$	2	V
$I_{PV,mpp}$	40	mA
V_{TEG}	500	mV
R_{TEG}	2	Ω
V_{PEH}	63.7	V
R_{PEH}	400	$k\Omega$
V_{BT}	3.7	V
P_{CZL}	30	mW
P_{CPL}	20-60	mW

The PV generator comprises two PV cells connected in series. The MPP of each cell occurs at the point (1 V, 40 mA) of the I-V curve. The built-in PSIM model of solar module is used. P&O MPPT algorithm is used to control the DC-DC buck-boost converter, as explained before. The block diagram which models MPPT method is shown in Figure 5. The reference voltage is $V_{MPP} = 2\ V$ and $\Delta V = 100\ mV$

A comercial thermoelectric cooler (TEC12706) is used in reverse mode as a TEG. The measured open circuit voltage for $\Delta T = 60\ K$ is approximately 500 mV. The parasitic resistance is equal to 2 $m\Omega$. For the PEH, considering the range of the parasitic elements discussed above, it is adopted $C_p = 25\ nF$ and $R_p = 1\ M\Omega$. The mechanical vibration frequency is $f = 25\ Hz$ and its amplitude is $I_p = 125\ \mu A$. From equations (2) and (3), it is possible to determine the parameters of the DC equivalent circuit shown in Table 2.

A buck-boost DC-DC converter with P&O MPPT algorithm is used to keep the output voltage of the device

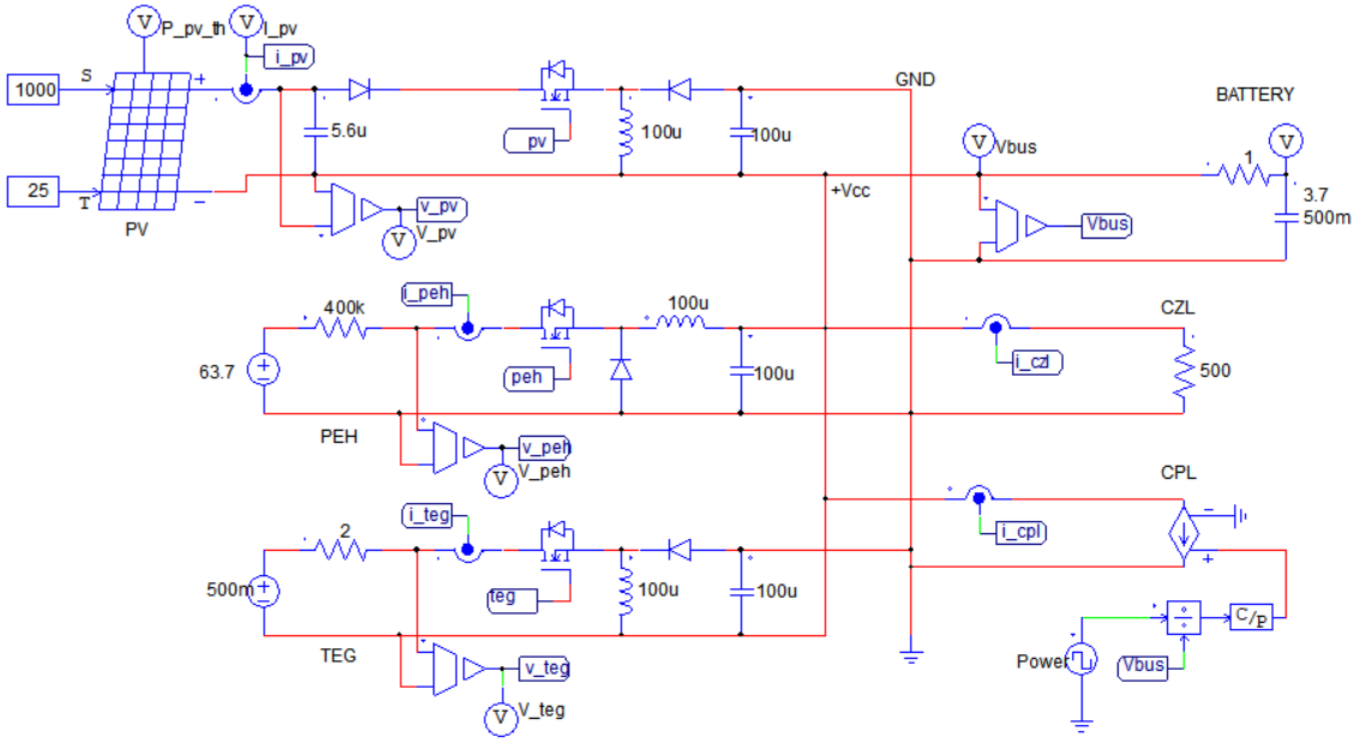

Figure 4. Circuit diagram of the proposed nanogrid model.

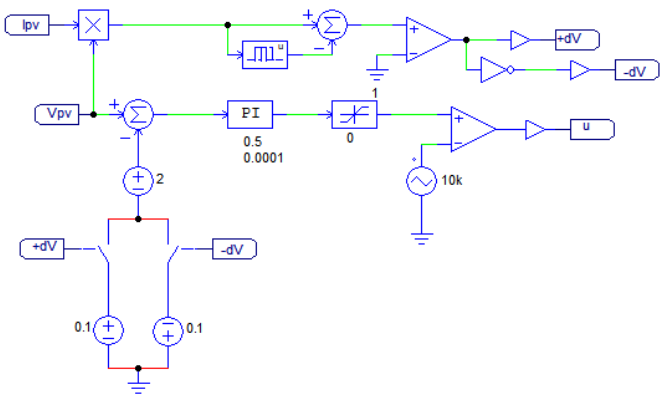

Figure 5. Schematic model of the P&O MPPT method.

around half of V_{oc}. The circuit is the same of the one used to control the PV converter, except for the reference voltage, which is half of the TEG open circuit voltage, i.e., 250 mV and $\Delta V = 12.5\ mV$. A Buck DC-DC converter with P&O MPPT is used to regulate the output voltage of PEH. In this case, a step down converter is used in order to reduce the voltage and properly connect to the DC bus. Analog to the TEG, the reference voltage on the P&O model is $V_{oc} = 31.85\ V$ and $\Delta V = 150\ mV$. The switching frequency of all DC-DC converters is 20 kHz.

A Li-Ion battery of 3.7 V is used as ESS of the system. Considering the complexity of the nanogrid, and the need for small simulation time step, the parameters of the battery was chosen so that the time constant of the equivalent RC circuit would be around 0.5 s. Furthermore, is considered that the battery is fully charged at the beginning of the simulation.

The constant power load is used to model electronic devices connected to the main bus. One is modeled to represent a power demand variation for the loads between 20 mW and 60 mW. It models, for example, the turning on of a small display or a sensor being switched on. A square wave was used to model this behavior. The resistive CZL of 1 $k\Omega$ models the equivalent resistive load as well as the ohmic losses on the nanogrid.

Despite the importance of a DC bus voltage control (Droop Control, Master-Slave, Distributed), the evaluation of any of those methods is not in the scope of this work.

4. SIMULATION RESULTS

The output voltage of each source at initial transient is shown on Figure 6. It is observed that the average value of the output voltages of the sources tend to their optimal values at steady state, i.e., $V_{PV} = 2\ V$ for the PV generator, and half of open circuit voltage for TEG and PEH, respectively, $V_{TEG} = 257\ mV$, $V_{PV} = 32.4\ V$.

The power delivered from sources at initial transient can be seen on Figure 7. It confirms that the maximum power is successfully tracked in all cases.

The behavior of the system considering different conditions is shown in Figure 8. On the upper graphic, the DC bus voltage is shown considering three different situations: (a) Battery only; (b) Battery, TEG, PEH and PV generation with 600 W/m^2 (*e.g* a cloudy day); (c) Battery, TEG, PEH and PV generation with 1000 W/m^2 (clear sky).

In case (a) DC bus (battery) voltage is reduced to about 95.68% of the initial state. In (b) voltage is reduced to 97.3%, and in (c) battery voltage is reduced to 98.92%. It is observed that the use of energy harvesting may prolong

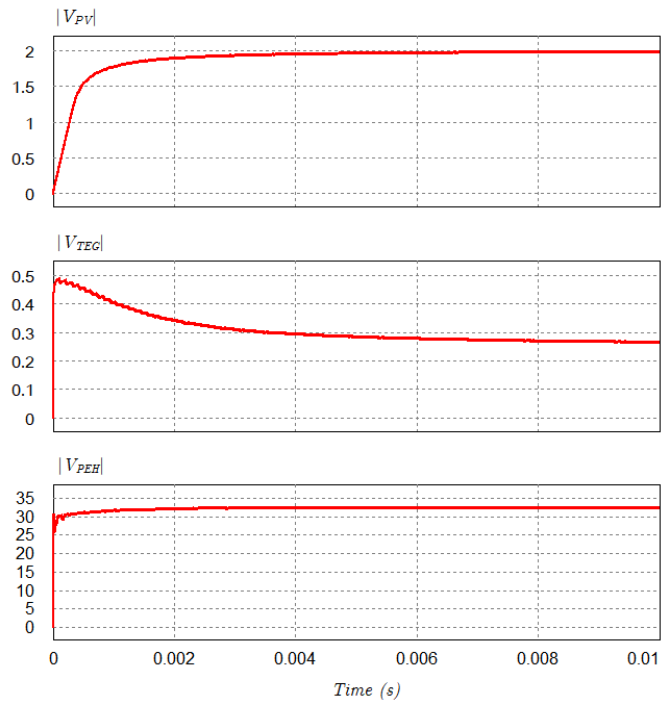

Figure 6. Output voltages of PV generator (top), TEG (middle), and PEH (bottom).

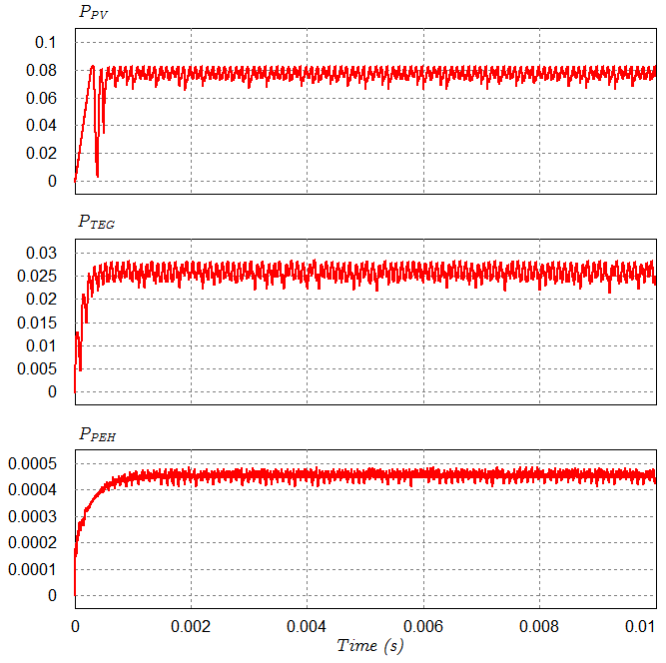

Figure 7. Delivered power from PV generator (top), TEG (middle), and PEH (bottom).

the battery discharge cycle or even reduce the volume of energy and consequently the size of the battery.

5. CONCLUSIONS

This work presented a proposal to integrate different sources of energy harvesting using a low power nanogrid concept. Simulation models of PV generators, thermoelectric generators and piezoelectric energy harvesters were presented.

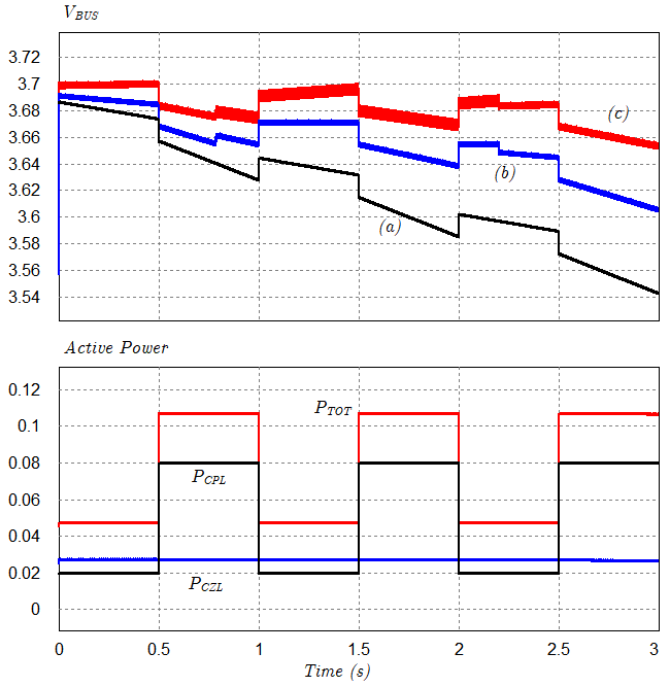

Figure 8. Main bus voltage (top) and demand load power (bottom).

Based on the described models, and on the addition of a battery and different types of loads, a nanogrid was modeled and simulated in PSIM. An increase in battery life has been observed as the reduction in terminal voltage is less intense with the use of the energy harvesting elements.

For future work, other types of MPPT methods, suitable design of the generation systems, analysis of the system under other types of disturbances and study of some of the DC bus voltage control methods may be included.

ACKNOWLEDGEMNTS

The authors would like to express their gratitude for the financial support offered by FAPEMIG, CNPq, CAPES, Federal University of Juiz de Fora and Federal Institute of Southeast of Minas Gerais.

REFERENCES

Bandyopadhyay, S. and Chandrakasan, A.P. (2012). Platform architecture for solar, thermal, and vibration energy combining with mppt and single inductor. *IEEE Journal of Solid-State Circuits*, 47(9), 2199–2215.

Bjørk, R. and Nielsen, K.K. (2015). The performance of a combined solar photovoltaic (pv) and thermoelectric generator (teg) system. *Solar Energy*, 120, 187–194.

Coelho, R.F., Concer, F.M., and Martins, D.C. (2010). Analytical and experimental analysis of dc-dc converters in photovoltaic maximum power point tracking applications. In *IECON 2010-36th Annual Conference on IEEE Industrial Electronics Society*, 2778–2783. IEEE.

Dell'Anna, F., Dong, T., Li, P., Yumei, W., Yang, Z., Casu, M.R., Azadmehr, M., and Berg, Y. (2018). State-of-the-art power management circuits for piezoelectric energy

harvesters. *IEEE Circuits and Systems Magazine*, 18(3), 27–48.

Do, X.D., Han, S.K., and Lee, S.G. (2014). Optimization of piezoelectric energy harvesting systems by using a mppt method. In *2014 IEEE Fifth International Conference on Communications and Electronics (ICCE)*, 309–312. IEEE.

Farret, F.A. and Simões, M.G. (2006). *Integration of Alternative Sources of Energy*. Wiley.

Hohm, D. and Ropp, M.E. (2003). Comparative study of maximum power point tracking algorithms. *Progress in photovoltaics: Research and Applications*, 11(1), 47–62.

Karami, N. and Moubayed, N. (2014). New modeling approach and validation of a thermoelectric generator. In *2014 IEEE 23rd International Symposium on Industrial Electronics (ISIE)*, 586–591. IEEE.

Nordman, B. (2013). Nanogrids: Evolving our electricity systems from the bottom up, building technology and urban systems department (btus). *Report, Berkeley Laboratory*.

Pozo, B., Garate, J.I., Araujo, J.Á., and Ferreiro, S. (2019). Energy harvesting technologies and equivalent electronic structural models. *Electronics*, 8(5), 486.

Raghunathan, V., Kansal, A., Hsu, J., Friedman, J., and Srivastava, M. (2005). Design considerations for solar energy harvesting wireless embedded systems. In *Proceedings of the 4th international symposium on Information processing in sensor networks*, 64. IEEE Press.

Ramadass, Y.K. (2009). *Energy processing circuits for low-power applications*. Ph.D. thesis, Massachusetts Institute of Technology.

Rezk, H. and Eltamaly, A.M. (2015). A comprehensive comparison of different mppt techniques for photovoltaic systems. *Solar energy*, 112, 1–11.

Shaikh, F.K. and Zeadally, S. (2016). Energy harvesting in wireless sensor networks: A comprehensive review. *Renewable and Sustainable Energy Reviews*, 55, 1041–1054.

Siouane, S., Jovanović, S., and Poure, P. (2017). Equivalent electrical circuits of thermoelectric generators under different operating conditions. *Energies*, 10(3), 386.